

# Eukaryotic Initiation Factor 2 $\alpha$ -independent Pathway of Stress Granule Induction by the Natural Product Pateamine A<sup>\*[5]</sup>

Received for publication, June 27, 2006, and in revised form, August 31, 2006. Published, JBC Papers in Press, September 2, 2006, DOI 10.1074/jbc.M606149200

Yongjun Dang<sup>‡</sup>, Nancy Kedersha<sup>§</sup>, Woon-Kai Low<sup>‡</sup>, Daniel Romo<sup>¶</sup>, Myriam Gorospe<sup>||</sup>, Randal Kaufman<sup>\*\*</sup>, Paul Anderson<sup>§</sup>, and Jun O. Liu<sup>‡###§§1</sup>

From the <sup>‡</sup>Department of Pharmacology and Molecular Sciences, <sup>\*\*</sup>Solomon H. Snyder Department of Neuroscience, and <sup>§§</sup>Department of Oncology, Johns Hopkins School of Medicine, Baltimore, Maryland 21205, <sup>§</sup>Division of Rheumatology and Immunology, Harvard Medical School, Brigham and Women's Hospital, Boston, Massachusetts 02115, <sup>¶</sup>Department of Chemistry, Texas A&M University, College Station, Texas 77842, <sup>||</sup>RNA Regulation Section, NIA, National Institutes of Health, Baltimore, Maryland 21224, and <sup>\*\*</sup>Howard Hughes Medical Institute, Departments of Biological Chemistry and Internal Medicine, University of Michigan Medical Center, Ann Arbor, Michigan 48109-0650

Stress granules are aggregates of small ribosomal subunits, mRNA, and numerous associated RNA-binding proteins that include several translation initiation factors. Stress granule assembly occurs in the cytoplasm of higher eukaryotic cells under a wide variety of stress conditions, including heat shock, UV irradiation, hypoxia, and exposure to arsenite. Thus far, a unifying principle of eukaryotic initiation factor 2 $\alpha$  phosphorylation prior to stress granule formation has been observed from the majority of experimental evidence. Pateamine A, a natural product isolated from marine sponge, was recently reported to inhibit eukaryotic translation initiation and induce the formation of stress granules. In this report, the protein composition and fundamental progression of stress granule formation and disassembly induced by pateamine A was found to be similar to that for arsenite. However, pateamine A-induced stress granules were more stable and less prone to disassembly than those formed in the presence of arsenite. Most significantly, pateamine A induced stress granules independent of eukaryotic initiation factor 2 $\alpha$  phosphorylation, suggesting an alternative mechanism of formation from that previously described for other cellular stresses. Taking into account the known inhibitory effect of pateamine A on eukaryotic translation initiation, a model is proposed to account for the induction of stress granules by pateamine A as well as other stress conditions through perturbation of any steps prior to the rejoining of the 60S ribosomal subunit during the entire translation initiation process.

Stress granules (SGs)<sup>2</sup> were first observed as cellular bodies visible by microscopy in tomato cells subjected to heat shock (1–3). Subsequently, SGs were identified in mammalian cells exposed to a variety of stress conditions, including oxidative stress, energy depletion, UV irradiation, and hypoxia (4). SG assembly is part of an adaptive response that recruits selected mRNAs and associated proteins for storage or triage to processing bodies (PBs) (5) that are sites of mRNA decay, allowing survival under adverse conditions. Sequestration of these components may help cells to recover post-stress by replenishing the cellular pool of mRNA without the need for new transcription. The physiological relevance of SGs is underscored by the presence of SGs in tissues of animals under stress (4), and SGs have been implicated in radioresistance of tumor cells (6) and tumor necrosis factor  $\alpha$  signaling (7). The study of SGs, their mechanism of formation, and biological role is a relatively new field in cell biology. Thus, a deeper understanding of the mechanism of SG formation and cellular functions may be clinically relevant.

A critical step in SG formation shared by most stress conditions is phosphorylation of the  $\alpha$  subunit of eukaryotic initiation factor 2 (eIF2) (8), which is a component of the eIF2-GTP-tRNAi<sup>Met</sup> ternary complex. The ternary complex is part of the 43S complex (40S particle, eIF3, and ternary complex) that is recruited to mRNA by the eIF4F complex (eIF4E, eIF4G, and eIF4A) during cap-dependent translation. The tRNAi<sup>Met</sup> of the ternary complex recognizes the AUG start codon prior to 60S subunit joining and 80S formation. Joining of 60S and release of initiation factors consumes two molecules of GTP, one of which is hydrolyzed by the ternary complex to generate eIF2-GDP (9). Phosphorylation of eIF2 $\alpha$  increases the affinity of eIF2B (an eIF2 GTP/GDP exchange factor) for eIF2-GDP by ~150-fold, sequestering the two proteins and inhibiting translation initiation (10). Ser-51 is the primary site of eIF2 $\alpha$  phos-

\* This work was supported by NCI, National Institutes of Health (NIH) and the Keck Foundation (to J. O. L.), NIH Grants A1033600 (to P. J. A. and N. L. K.) and DK42394 (to R. J. K.), and a Canadian Institutes of Health Research fellowship (to W. K. L.). The costs of publication of this article were defrayed in part by the payment of page charges. This article must therefore be hereby marked "advertisement" in accordance with 18 U.S.C. Section 1734 solely to indicate this fact.

[5] The on-line version of this article (available at <http://www.jbc.org>) contains supplemental Figs. S1–S3.

<sup>1</sup> To whom correspondence should be addressed: Dept. of Pharmacology and Molecular Sciences, Johns Hopkins School of Medicine, Hunterian 516, 725 N. Wolfe St., Baltimore, MD 21205. Tel.: 410-955-4619; Fax: 410-955-4620; E-mail: joliu@jhu.edu.

<sup>2</sup> The abbreviations used are: SG, stress granule; PatA, pateamine A; B-PatA, biotin-PatA; CHX, cycloheximide; DMDA-PatA, desmethyl, desamino PatA; Me<sub>2</sub>SO, dimethyl sulfoxide; EMCV, encephalomyocarditis virus; IRES, internal ribosome entry site; PB, processing body; MEF, mouse embryonic fibroblast; eIF, eukaryotic initiation factor; PBS, phosphate-buffered saline; DTT, dithiothreitol; TIA-1, T cell intracellular antigen-1; TIAR, TIA-1 related; SH3, Src homology 3.

phorylation, which can be phosphorylated by several kinases, including the heme-regulated eIF2 $\alpha$  kinase, double-stranded RNA-activated protein kinase, the endoplasmic reticulum-localized eIF2 $\alpha$  kinase, and GCN2 under different stress conditions (4). The generally accepted model is that phosphorylation of eIF2 $\alpha$  is necessary and sufficient for SG assembly (11), which is supported by several lines of evidence that include: 1) Overexpression of an eIF2 $\alpha$  (S51A) mutant blocked SG assembly (12); 2) Expression of a phosphomimetic eIF2 $\alpha$  (S51D) mutant was sufficient to induce SG formation (12); and 3) eIF2 $\alpha$ /S51A knock-in MEFs were not able to assemble SGs upon exposure to arsenite, heat shock, or carbonyl cyanide *p*-trifluoromethoxyphenylhydrazone, but eIF2 $\alpha$ /S51A mutant cells overexpressing eIF2 $\alpha$ /S51D were capable of SG assembly under the same conditions (11, 13). Aside from eIF2 $\alpha$ , several other protein factors have been shown to regulate SG assembly downstream of eIF2 $\alpha$ , including T cell intracellular antigen-1 (TIA-1) (14, 15) and Ras-GAP-SH3-binding protein (G3BP) (16).

We and others have recently reported that the marine sponge natural product, pateamine A (PatA), can inhibit translation initiation through interaction with eIF4A (17, 18). Although the binding of PatA to eIF4A stimulates its intrinsic ATPase and RNA helicase activity, the underlying cause of inhibition of translation initiation is likely due to the disruption of the eIF4F complex (18). A closely related analog of slightly lower potency, desmethyl, desamino PatA (DMDA-PatA) acts by a similar mechanism, and a precursory investigation suggested that both compounds were capable of inducing SGs (18). In this study, we have demonstrated that the cellular bodies observed under PatA (or DMDA-PatA) treatment are similar to the SGs induced by arsenite in terms of composition and dynamic assembly. However, PatA induces SGs independent of eIF2 $\alpha$  phosphorylation, in contrast to other SG-inducing stress conditions or agents characterized thus far. Additionally, unlike arsenite, PatA was unable to induce the formation of PBs, which are sites of mRNA decay (5).

## EXPERIMENTAL PROCEDURES

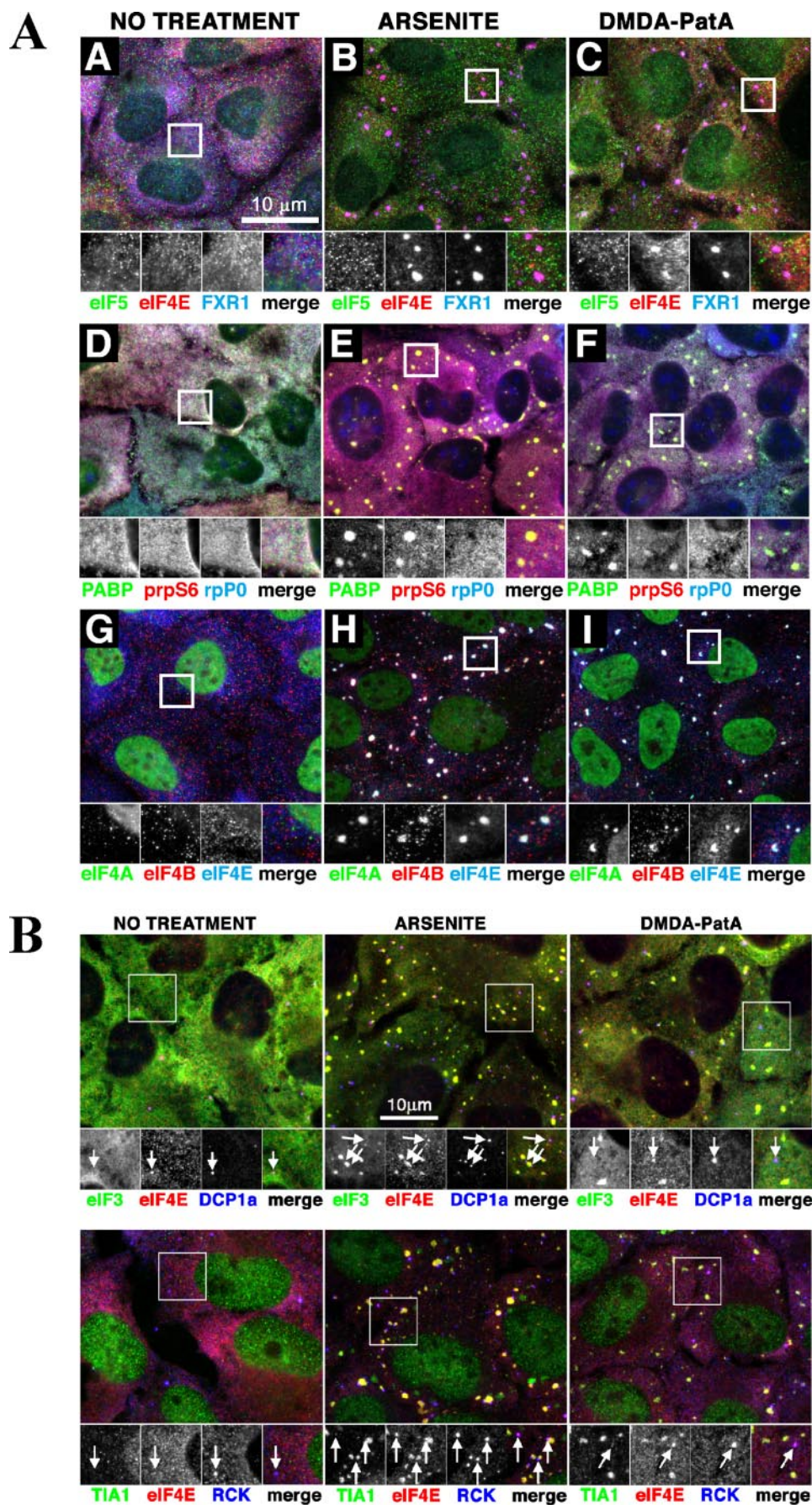
**Cell Lines and Reagents**—PatA, DMDA-PatA, and Biotin-PatA were synthesized as previously reported (18, 19). Sodium arsenite, cycloheximide (CHX), and 5'-guanylyl-imidodiphosphate were purchased from Sigma-Aldrich. Antibodies were purchased from commercial sources: antibodies against eIF4A1 (sc-14221, goat), eIF4E (sc-9976, mouse), FXR1 (sc-10544), eIF3p116 (sc-16377, goat), ribosome L28 (sc-14151, goat), TIA-1 (sc-1751, goat), TIAR (sc-1749, goat), eIF5 (sc-282, rabbit), PABP (sc-32318, mouse), and horseradish peroxidase-conjugated secondary antibodies (Santa Cruz), anti-FLAG (Sigma-Aldrich), antibodies against eIF2 $\alpha$ , (9722, rabbit) eIF4B (3592, rabbit), and ribosome S6 and phospho-S6 (Cell Signaling Technology), anti-eIF4G (BD Transduction), anti-phospho-eIF2 $\alpha$  (StressGen Biotechnologies Corp.), human autoantiserum against ribosomal P0 antigen (ImmunoVision, Springdale, AR), Cy2-, Cy3-, and Cy5-conjugated secondary antibodies (ML grade for multiple labeling; Jackson ImmunoResearch). Alex488-conjugated streptavidin was from Invitrogen. TIA-1 and TIAR oligo small interference RNA was generated as pre-

viously reported (20, 21). Other reagents were generously provided by Dr. Jens Lykke-Anderson (hDcp1a antibody) and Dr. David Ron (eIF2 $\alpha$  and mutants, which were subcloned into the pCMVTag2B vector; Stratagene). HeLa cells and U2-OS cells were cultured in Dulbecco's modified Eagle's medium plus 10% fetal bovine serum at 5% CO<sub>2</sub>. eIF2 $\alpha$  mutant (S51A) and wild-type MEF cell lines were generated as previously reported (22).

**Immunofluorescence**—Immunofluorescence was performed using antibodies according to the manufacturer's instructions or as described previously (12, 23). Briefly, cells were plated on coverslips and allowed to recover for 16–24 h. In Fig. 3B, cells were transfected with indicated plasmids or oligo small interference RNA and treated as indicated for 48 h. Cells were fixed with 4% *p*-formaldehyde for 15 min. The cells were washed in PBS, permeabilized by 0.5% Triton X-100 or –20 °C methanol, and blocked with 10% donkey serum in PBS prior to 1 h of incubation with combinations of primary antibodies raised in different host species as indicated in the figure legends. Cells were incubated in three changes of PBS for 5 min each and then incubated in secondary antibody cocktails (e.g. a mixture of donkey anti-goat Cy2 at 1/200, donkey anti-mouse Cy3 at 1/2000, and donkey anti-rabbit Cy5 at 1/200) containing 4',6-diamidino-2-phenylindole made in blocking buffer and incubated for 1 h. Cells were then washed three times in PBS for 5 min, mounted, viewed, and photographed. Mounting was performed using Vectashield mounting medium (Vector Laboratories), and images were captured using either a Zeiss LSM510 confocal microscope (Figs. 2 and 3B and supplemental Figs. S1 and S3) or a Nikon Eclipse E800 microscope and photographed using a National Diagnostics CCD-SPOT RT camera. (Figs. 1, 3C, and 4 and supplemental Fig. S2). Merged images were compiled using LSM5 Image Examiner or Adobe Photoshop CS. Data obtained from the green/Cy2 channel are shown *green*, the red/Cy3 data are shown *red*, and data from the far-red/Cy5 channel are shown in *blue*.

**In Vitro Transcription and Translation**—Dual luciferase plasmids containing hepatitis C virus or encephalomyocarditis virus (EMCV) internal ribosome entry sites (IRES) (24) were linearized by BamHI and transcribed using T7 polymerase (Promega). Translation was performed using the Flexi<sup>®</sup> rabbit reticulocyte lysate (RRL) system (Promega). Briefly, 200 ng of RNA was combined in 20- $\mu$ l reactions containing 10  $\mu$ l of rabbit reticulocyte lysate, 0.2  $\mu$ l each of –Met and –Leu amino acid mixtures, 70 mM KCl, 2 mM DTT, and 10 units of RNasin (Promega) with the indicated concentration of arsenite. Reaction mixtures were incubated at 30 °C for 1.5 h. A 5- $\mu$ l aliquot was assayed for luciferase activity according to the instructions of the manufacturer (Dual-Luciferase<sup>®</sup> reporter assay system; Promega).

**Sucrose Gradient Density Centrifugation**—200 ng of radiolabeled, capped  $\beta$ -globin RNA was combined with 25  $\mu$ l of rabbit reticulocyte lysate, 0.4  $\mu$ l each of –Met and –Leu amino acid mixtures (Promega), 10 units of RNasin, 70 mM KCl, and 2 mM DTT in a total volume of 40  $\mu$ l. The resultant mixtures were incubated at 30 °C for 15 min, diluted with 160  $\mu$ l of gradient buffer (20 mM HEPES, pH 7.4, 150 mM KC<sub>2</sub>H<sub>3</sub>O<sub>2</sub>, 5 mM MgCl<sub>2</sub> and 1 mM DTT), and overlaid onto 15–35% (w/v) linear sucrose gradients that were subjected to ultracentrifugation at 50,000



rpm in a Beckman SW55i rotor at 4 °C for 1 h. Fractions (200  $\mu$ l) were manually collected from the top of the gradient, and the amount of radiolabeled RNA in each fraction was determined by scintillation counting.

**Cellular Polysome Profiles**—eIF2 $\alpha$ /S51A mutant and wild-type cells were treated as indicated for 60 min. Cells were washed twice with ice-cold PBS and lysed in 500  $\mu$ l of chilled TMK100 buffer (20 mM Tris-HCl, pH 7.4, 5 mM MgCl<sub>2</sub>, 100 mM KCl, 2 mM DTT, 1% Triton X-100, 100 units/ml RNasin (Promega), and protease inhibitors (Roche Diagnostics) in diethyl pyro-carbonate-treated water. After clearing at 10,000  $\times$  g (10 min) at 4 °C, the supernatants (S10) were layered onto 10-ml, 15–45% linear sucrose gradients containing 20 mM HEPES, pH 7.4, 100 mM KCl, 5 mM MgCl<sub>2</sub> and 2 mM DTT. Ultracentrifugation at 40,000 rpm for 2 h at 4 °C was performed in a SW41Ti rotor (Beckman). Gradient profiles were monitored at 254 nm from the top of the gradient by injection of Flurnert FC-40 from the bottom of the centrifuge tube.

## RESULTS

**SGs Induced by DMDA-PatA and Arsenite Are Similar in Composition**—To date, a number of core protein components of SGs have been identified using immunofluorescence (2–4, 12). To validate that the cellular bodies formed by PatA treatment are *bona fide* SGs, cells were treated with either the classical SG inducer arsenite or with DMDA-PatA and then processed for immunofluorescence using a panel of antibodies directed against SG marker proteins (Fig. 1A). Known SG markers eIF4E, Fragile X-related protein 1 (FXR1), poly(A)-binding protein 1 (PABP1), small ribosomal subunit protein S6 protein, eIF4A, and eIF4B were all localized to SGs upon treatment of U2-OS cells with either DMDA-PatA or arsenite. Conversely, SGs induced by either stimulus did not contain the large ribosome subunit protein P0 (Fig. 1A, panels E and F, blue) and L28 (supplemental Fig. S1) or eIF5 (Fig. 1A, panels B and C, green). This analysis indicates that arsenite and PatA induce SGs of similar composition.

**DMDA-PatA Does Not Induce PBs**—To determine whether PatA treatment induces PBs in addition to SGs, U2-OS cells were treated with DMDA-PatA and compared with cells treated with arsenite, which has been shown to induce both SGs and PBs, which are frequently juxtaposed (23). SGs were detected using antibodies against eIF3b (Fig. 1B, top row, green) or TIA-1 (bottom row, green), while both SGs and PBs were visualized using antibodies against their common protein eIF4E (Fig. 1B, red). Two independent PB markers, the decapping protein DCP1a (top row, blue) and p54/RCK (bottom row, blue), were used to assess PB formation. As expected, arsenite treatment (middle panels) induced both SG (green) and PB forma-

tion (blue), causing a 5-fold increase in PBs, which appear purple in the merged views, some of which are indicated by white arrows in the insets. However, a comparison arsenite treatment (middle panels) to DMDA-PatA treatment (right panels) revealed that only arsenite induced PB formation, whereas DMDA-PatA treatment caused no increase in PBs despite its ability to induce SG assembly.

**Dynamic SG Formation and Localization of PatA within SGs**—The formation of SGs is highly dynamic, and SGs are fully reversible upon removal of stress conditions, with many components including mRNA shuttling between SGs, polysomes, and other RNA granules such as PBs (11, 23). When HeLa cells were treated with arsenite, PatA, or DMDA-PatA, SGs were observed within 30 min (Fig. 2A, row 1). For cells that were washed with PBS and allowed to recover in complete growth medium, SGs were no longer detectable in arsenite-treated cells but remained visible in both DMDA-PatA and PatA-treated cells (Fig. 2A, row 2). Elongation inhibitors emetine and CHX stabilize polysomes by inhibiting elongating ribosomes and inhibit SG assembly (14). By allowing cells to recover in the presence of CHX, SGs were disassembled in cells treated with PatA or DMDA-PatA, similar to arsenite (Fig. 2A, row 3), and pretreatment of cells with CHX for 30 min completely blocked SG formation in response to stimulation by all compounds (Fig. 2A, row 4).

We have previously shown that PatA binds to eIF4AI(II), promoting the formation of the complex between eIF4AI(II) and eIF4B (18). As both eIF4AI(II) and eIF4B also localize into SGs under PatA treatment, we determined whether PatA is also incorporated into SGs. The availability of a biotin-conjugated PatA (B-PatA) (18) allows for indirect immunofluorescence detection of B-PatA using streptavidin conjugated to Alexa 488. B-PatA was able to induce SGs similar to DMDA-PatA, as judged by immunofluorescence detection of the SG marker TIA-1, and importantly, B-PatA was concentrated within SGs as determined by co-localization with TIA-1 (Fig. 2B). Together, these results indicate that formation of PatA-induced SGs is dynamic and that PatA (and likely its analogs) is incorporated into SGs.

**eIF2 $\alpha$  Phosphorylation Is Not Required for PatA-induced SGs**—The phosphorylation of eIF2 $\alpha$  at Ser-51 has been shown to play a critical role in the inhibition of protein synthesis and induction of SG formation by arsenite (4). The phosphorylation status of eIF2 $\alpha$  was determined by immunoblotting of lysates from HeLa cells treated with DMDA-PatA, arsenite, or Me<sub>2</sub>SO (mock) (Fig. 3A). Arsenite dramatically induced the phosphorylation of eIF2 $\alpha$  as previously reported (12). In contrast,

**FIGURE 1. DMDA-PatA treatment induces stress granules with similar composition as those induced by arsenite but does not induce processing bodies.** A, U2-OS cells were untreated (A, D, G), exposed to 500  $\mu$ M arsenite for 45 min (B, E, H) or 50 nM DMDA-PatA for 45 min (C, F, I), and then fixed and probed with indicated antibodies. A–C, cells stained for eIF5 (rabbit polyclonal, green), eIF4E (mouse monoclonal, red), and FXR1 (goat polyclonal, blue). D–F, cells stained for PABP-1 (mouse monoclonal, green), ribosomal protein S6 (rabbit polyclonal, red), and large ribosomal protein P0 (human autoantiserum, blue). G–I, cells stained for eIF4A (goat polyclonal, green), eIF4B (rabbit polyclonal, red), and eIF4E (mouse monoclonal, blue). Enlarged views of the boxed regions are shown as separate grayscale panels and as a merged image at the bottom of each panel. B, U2-OS were treated as in panel A and then fixed and stained as indicated. Top row, eIF3b (goat polyclonal, green), eIF4E (mouse monoclonal, red), and DCP1a (rabbit polyclonal, blue). Bottom row, TIA-1 (goat polyclonal, green), eIF4E (mouse monoclonal, red), and p54/RCK (rabbit polyclonal, blue). Enlarged views of the boxed regions showing separate and merged views are shown at the bottom of each corresponding panel. Bar, 10  $\mu$ m. The arrows indicate the position of PBs, which are not stained by all antibodies (eIF3, TIA-1) and do not appear in all panels.

## Pateamine A Induction of Stress Granules

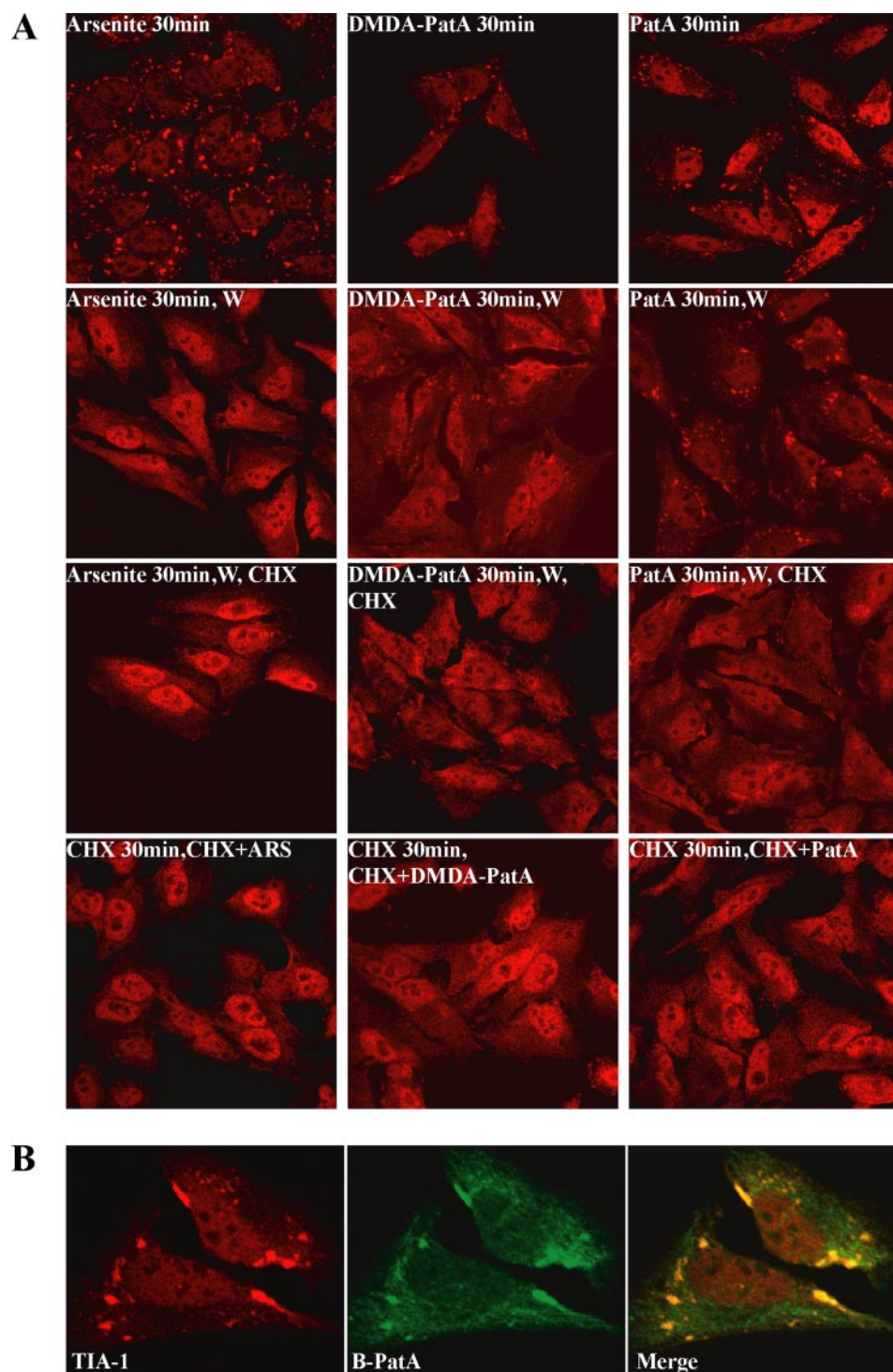


**FIGURE 2. PatA-induced SGs are dynamic, and B-PatA is incorporated into SGs.** HeLa cells were treated with drugs as indicated and stained with TIA-1-specific antibody. *A*, HeLa cells were treated with arsenite (500  $\mu$ M), DMDA-PatA (50 nM), or PatA (50 nM) for 30 min (row 1), followed by washing with PBS (indicated by *W*). The cells were then cultured in complete growth medium in the presence or absence of CHX (100  $\mu$ g/ml) for 1 h (rows 2 and 3). Cells were pretreated with 100  $\mu$ g/ml CHX for 30 min, followed by treatment with either arsenite, DMDA-PatA, or PatA for 1 h (row 4). *B*, HeLa cells were treated with B-PatA (200 nM) for 3 h and stained with antibody against TIA-1 (red) or streptavidin-Alexa 488 (green).

DMDA-PatA did not induce phosphorylation of eIF2 $\alpha$  in comparison with control.

The overexpression of a S51A mutation of eIF2 $\alpha$  has been demonstrated to inhibit SG formation induced by arsenite (8), and SG assembly does not occur when MEFs that harbor a S51A

knock-in mutation in the eIF2 $\alpha$  gene are exposed to arsenite (8, 11). It was found that overexpression of the S51A eIF2 $\alpha$  mutant had no effect on SG formation in the presence of DMDA-PatA, even though it prevented SG formation caused by arsenite (Fig. 3*B*). To further confirm the independence of DMDA-PatA-induced SG formation from eIF2 $\alpha$  phosphorylation, we examined SG induction in eIF2 $\alpha$ /S51A mutant and wild-type MEFs. Treatment of wild-type cells with either arsenite or DMDA-PatA resulted in the formation of SGs (Fig. 3*C* or supplemental Fig. S2). In the eIF2 $\alpha$ /S51A mutant cells, arsenite was unable to induce SG formation as previously described (11). However, DMDA-PatA treatment induced the formation of SGs in the eIF2 $\alpha$ /S51A mutant MEFs similar to wild-type cells. Another noticeable difference between DMDA-PatA and arsenite was that in wild-type MEFs, arsenite-induced SGs did not contain eIF2 $\alpha$ , whereas eIF2 $\alpha$  was localized to SGs induced by DMDA-PatA in both wild-type and eIF2 $\alpha$ /S51A mutant cells (Fig. 3*C*). These results unambiguously demonstrate that SG formation induced by DMDA-PatA is independent of eIF2 $\alpha$  phosphorylation.

*TIA-1/R Response Downstream of Stalled Initiation Is Similar between PatA and Arsenite*—TIA-1/R act downstream of phospho-eIF2 $\alpha$  to potentiate SG assembly through self-aggregation (8). When each protein was individually knocked down with oligo small interference RNA in HeLa cells, there was no effect on SG assembly induced by either DMDA-PatA or arsenite (supplemental Fig. S3). Furthermore, no differences between the two compounds were observed in TIA-1 or TIAR knock-out MEFs (Fig. 4). Loss of TIA-1 or TIAR individually did not prevent SG formation, likely due to compensation of

function by the other protein. While stalled 48S complexes are the core units of SGs, the size and stability of SGs likely also depend on the abundance and activity of the many self-aggregating mRNA-binding proteins known to facilitate SG assembly, *e.g.* TIA-1, TIAR, TTP, and G3BP (4). However, TIA-1

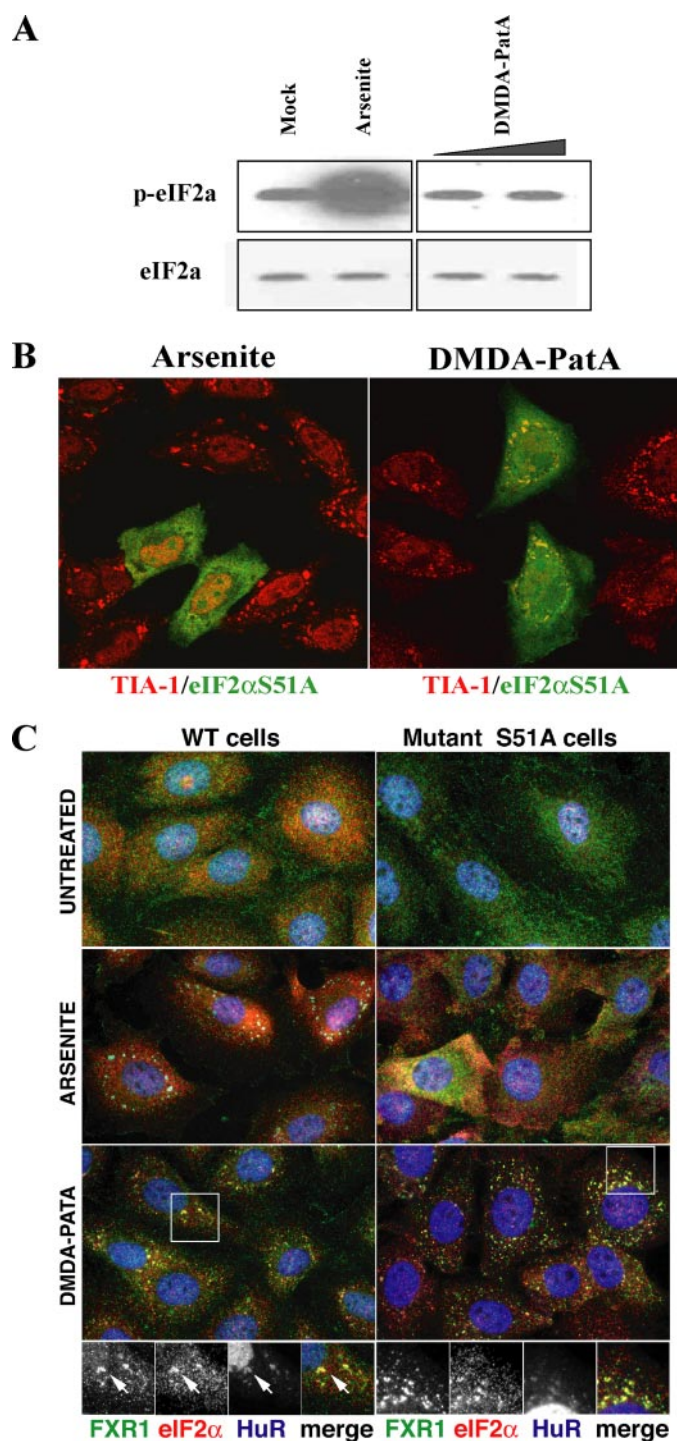


**FIGURE 3. Stress granule induction by DMDA-PatA is independent of eIF2 $\alpha$  phosphorylation.** *A*, HeLa cells were treated with either Me<sub>2</sub>SO (mock), 300  $\mu$ M arsenite, 50 nM DMDA-PatA, or 1  $\mu$ M DMDA-PatA for 1 h, and eIF2 $\alpha$  phosphorylation status was determined by immunoblotting using phospho-eIF2 $\alpha$  and eIF2 $\alpha$ -specific antibodies. *B*, plasmid encoding FLAG-eIF2 $\alpha$ S51A was transiently transfected into HeLa cells as indicated. After 48 h, cells were treated with arsenite (300  $\mu$ M) or DMDA-PatA (50 nM) for 1.5 h before they were fixed and stained with TIA-1 and FLAG tag-specific antibodies for immunofluorescence detection. *C*, wild-type or eIF2 $\alpha$  S51A mutant MEFs were treated with Me<sub>2</sub>SO (top row), 500  $\mu$ M arsenite (middle row), or 50 nM DMDA-PatA (bottom row) for 45 min. The cells were fixed and stained for FXR1 (goat polyclonal, green), eIF2 $\alpha$  (rabbit polyclonal, red), and HuR (mouse monoclonal, blue). Insets are enlarged views showing separate and merged color channels. The arrows indicate the position of an SG.

knock-out MEFs evinced a muted SG response to both arsenite and DMDA-PatA by assembly of smaller SGs, whereas TIAR knock-out MEFs readily assembled larger SGs in response to both compounds (Fig. 4). We previously reported that arsenite-induced SGs are smaller in TIA-1 knock-out MEFs, whereas TIAR knock-out MEFs exhibit enhanced SG assembly (15) similar to those observed for DMDA-PatA (Fig. 4).

*In Vitro Inhibition of Translation Initiation by Arsenite Is Distinct from PatA*—As arsenite inhibits translation and induces SGs *in vivo* (8), we examined the effect of arsenite on translation initiation *in vitro* using bicistronic luciferase (Firefly and *Renilla*) reporter vectors, where the first cistron was translated by cap-dependent initiation and the second cistron was controlled by either the EMCV or the hepatitis C virus IRES (24). As shown in Fig. 5A, all cap-dependent translation and translation initiated from both IRES elements were inhibited by arsenite. Furthermore, sucrose gradient analysis of translation initiation complexes with radiolabeled  $\beta$ -globin RNA (25) revealed that arsenite caused a slight accumulation of 48S complexes as compared with control, although significant amounts of 80S particles bound to RNA were also detected (Fig. 5B). Co-treatment with CHX did not affect the arsenite profile. However, co-treatment with 5'-guanylyl-imidodiphosphate caused the disappearance of the 80S peak and an enhanced 48S peak, a profile similar to 5'-guanylyl-imidodiphosphate alone (Fig. 5B). This *in vitro* effect of arsenite is similar to that for PatA (18). However, the lack of discrimination between hepatitis C virus and EMCV IRES-mediated translation initiation distinguishes arsenite from PatA, which only inhibited EMCV IRES (18).

*In vivo* polysome profiles have been useful in describing arsenite effects and observing changes in polysome content (11). For wild-type MEFs, both arsenite and DMDA-PatA caused the depletion of polysomes and the appearance of a large peak at the "80S" position as previously observed. For eIF2 $\alpha$ /S51A mutant MEFs, arsenite treatment caused a significant perturbation of the polysome region. However, some polysomes, albeit fewer, still remained. In contrast, DMDA-PatA caused nearly complete depletion of polysomes and the appearance of the apparent "80S" peak in the eIF2 $\alpha$ /S51A mutant MEFs. The inability of arsenite to completely deplete the polysome profile of eIF2 $\alpha$ /S51A mutant MEFs and the essentially identical results for both eIF2 $\alpha$ /S51A mutant and wild-type MEFs for PatA corroborate the earlier observation that eIF2 $\alpha$  phosphorylation is required for SG induction by arsenite, but not by PatA.

## DISCUSSION

In this study, we employed the natural product PatA and its analogs, DMDA-PatA and B-PatA, which were recently shown to induce SGs (18), as probes to investigate the mechanism of SG assembly. Arsenite induces SGs through activation of heme-regulated eIF2 $\alpha$  kinase, which phosphorylates eIF2 $\alpha$  at Ser-51 (11). Using arsenite as a control compound we have effectively demonstrated that the induction of SGs by PatA is not dependent on the phosphorylation of eIF2 $\alpha$ . To date, the only reported cases where SG formation has not been clearly linked with eIF2 $\alpha$  phosphorylation involves acute energy starvation

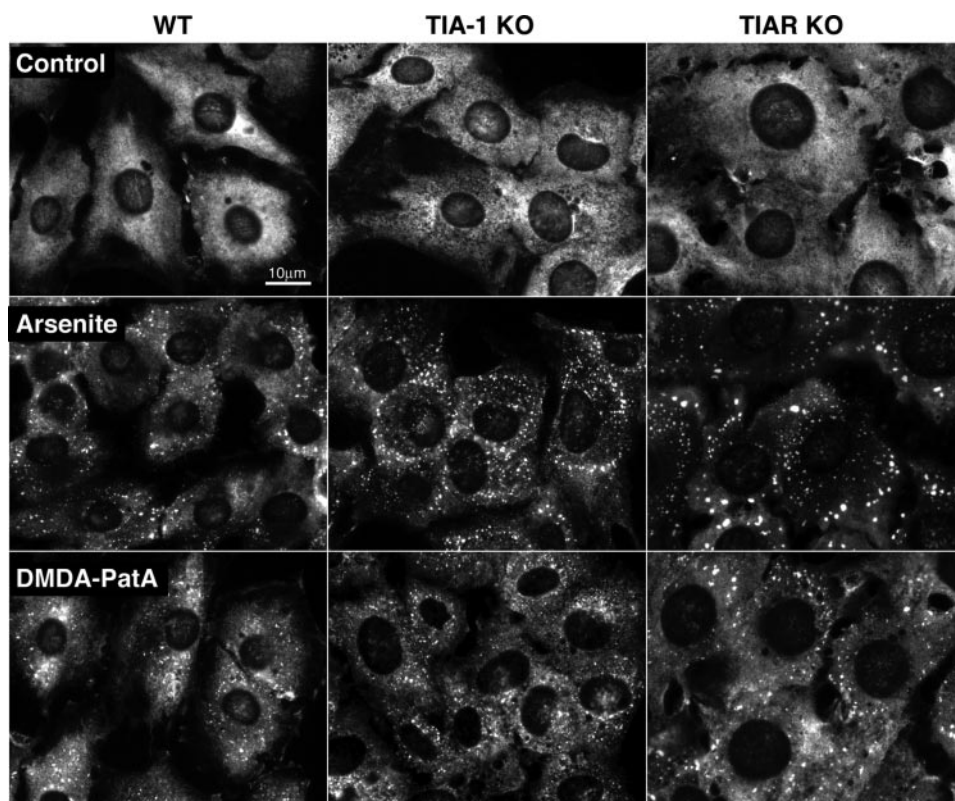


FIGURE 4. **SGs induced by DMDA-PatA in TIA-1 and TIAR knock-out MEFs.** Cells were treated with either  $\text{Me}_2\text{SO}$  (top row),  $500 \mu\text{M}$  arsenite (middle row), or  $50 \text{ nM}$  DMDA-PatA (bottom row) for 45 min before they were fixed and stained for the SG marker protein eIF3b.

induced by glucose deprivation, treatment with the mitochondrial poison carbonyl cyanide *p*-trifluoromethoxyphenylhydrazone in DU145 cells (12), or treatment with the hexokinase inhibitor clotrimazole (11). However, none of these stimuli induces SGs in eIF2 $\alpha$ /S51A mutant MEFs, suggesting that a basal level of eIF2 $\alpha$  phosphorylation is required (11). Accordingly, previous models all suggested that eIF2 $\alpha$  phosphorylation was an essential prerequisite to SG formation (4). Our results presented here clearly demonstrate an instance where SG assembly is not dependent on eIF2 $\alpha$  phosphorylation, shedding new light on the mechanism of SG formation.

The fact that the majority of data accumulated to date have implicated the phosphorylation of eIF2 $\alpha$  as a necessary step for SG formation raises the question of whether the granules induced by PatA and its analogs are indeed true SGs. Other notable differences between PatA and arsenite included a delayed rate of disassembly, eIF2 localization within SGs, and lack of PB induction for PatA. The inability of cells to recover from PatA or DMDA-PatA treatment by simple washing of cells and recovery in complete growth medium would indicate that SGs induced by PatA are more stable than those induced by arsenite. However, the demonstration of identical core components examined and the dynamic assembly-disassembly of SGs induced by PatA, albeit with a slower rate of disassembly than that observed for arsenite-induced SGs, suggest that SGs formed in the presence of PatA are still fundamentally similar to SGs described for other stresses. Furthermore, the identical responses to TIA-1/R knock down and responses of the TIA-1/R knock-out MEFs to both DMDA-PatA and arsenite would

also indicate that PatA-induced SGs are likely *bona fide* SGs. The differential localization of eIF2 (excluded from SGs for arsenite and included in SGs for PatA) is consistent with arsenite-induced SGs being dependent on eIF2 $\alpha$  phosphorylation. For arsenite, phosphorylation of eIF2 $\alpha$  reduces the availability of the ternary complex, thereby inhibiting translation initiation (8). SGs are aggregates of stalled initiation complexes; thus, the lack of ternary complex formation would exclude eIF2 from the stalled initiation complexes, causing their absence from SGs. However, incorporation of eIF2 $\alpha$  into PatA-induced SGs suggests that ternary complexes are formed, are part of the 43S complex, and thus become incorporated into SGs. The differences in PB formation may be unrelated to the general mechanism of SG assembly and may be arsenite specific, as clotrimazole and heat shock also do not induce PBs (23). Thus, PatA-induced SGs are very similar in composition to SGs induced by arsenite, even

though their mechanisms of formation differ.

*In vitro*, PatA inhibits translation initiation by perturbing eIF4F function. However, a discrepancy exists in the reported experimental evidence. In one study (17), PatA prevented the formation of 48S complexes by blocking the association of 43S with RNA. In our previous work (18), PatA did not perturb 43S joining to RNA but caused the stalling of the 48S complex with severely delayed 80S formation. Direct incorporation of B-PatA into SGs, likely through eIF4A interaction, may account for the greater stability of PatA-SGs and the inability to recover cells by washing with PBS. The presence of B-PatA within SGs also suggests that, *in vivo*, PatA and its analogs are incorporated into stalled 48S complexes. SG assembly appears to occur in two distinct phases, the abortive initiation event leading to accumulation of 48S complexes and the aggregation of these complexes into SGs that cycle through an assembly-disassembly process. Furthermore, we have previously proposed an offshoot pathway that re-routes selected mRNA for degradation (PB formation) under arsenite treatment (23). The lack of PB induction by PatA may suggest that this pathway is either blocked or not induced for SGs formed in the presence of PatA. Thus, the effects upstream of SG assembly, *i.e.* eIF2 $\alpha$  phosphorylation status, and the downstream effects, PB assembly, differ for PatA and arsenite, but the core assembly-disassembly process for SGs remains consistent.

The recruitment of the ternary complex to the 40S ribosomal subunit is not the site of PatA action, which directly disrupts the eIF4F complex. Arsenite has several cellular effects such as protein misfolding (26), impairment of the ubiquitin-proteasome

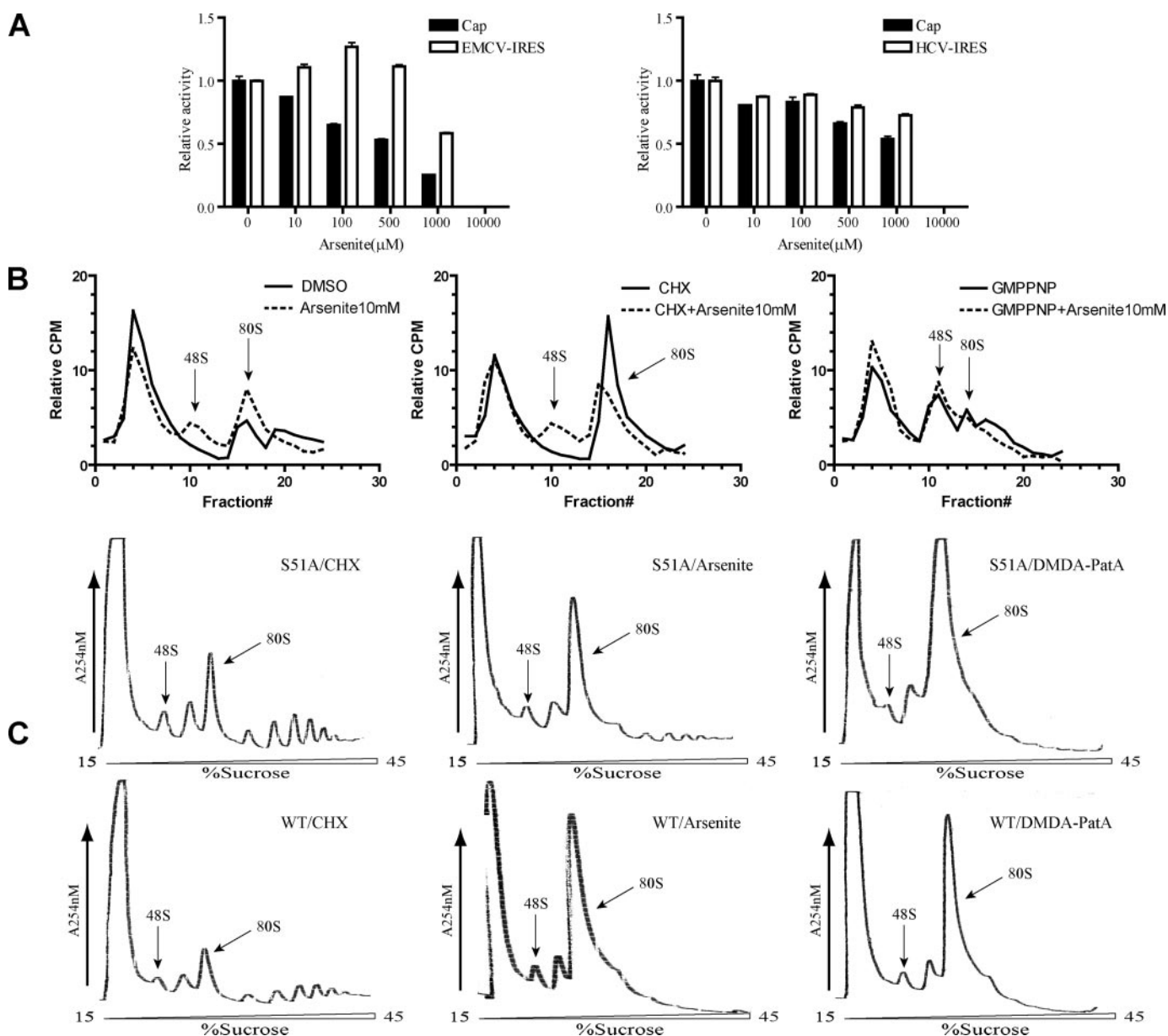


**FIGURE 5. Arsenite inhibits translation at the initiation step.** *In vitro* protein translation was quantified by determination of luciferase activity translated from bicistronic reporter RNAs, with the first cistron encoding Firefly luciferase and the second cistron encoding *Renilla* luciferase. *A*, solid bars represent cap-dependent (1st cistron) activity, and clear bars represent respective IRES (2nd cistron) activity. Readings were taken in triplicate, and error bars represent  $\pm 1$  S.D. *Right*, cap-dependent versus hepatitis C virus IRES-dependent translation under arsenite treatment. *Left*, cap-dependent versus EMCV IRES-dependent translation under arsenite treatment. *B*, 48S and 80S particles bound to radiolabeled capped  $\beta$ -globin in the presence of arsenite alone (10 mM) or in combination with CHX (0.75 mM) or 5'-guanylyl-imidodiphosphate (1.25 mM) were resolved by sucrose density gradient centrifugation followed by fractionation and scintillation counting. *C*, polyribosome profiles determined from eIF2 $\alpha$ /S51A mutant and wild-type cells after 1 h of treatment with 100  $\mu$ g/ml CHX, 300  $\mu$ M arsenite, or 50 nM DMDA-PatA.

pathway (27), oxidative stress, and impairment of several signaling pathways (28–30), with downstream heme-regulated eIF2 $\alpha$  kinase activation leading to eIF2 $\alpha$  phosphorylation. As such, it is not surprising that PatA is able to induce SG formation without phosphorylating eIF2 $\alpha$ . Accordingly, we surmise that any factor or incident that prevents 40S, and its associated factors, from forming a translationally competent 80S particle can induce SGs. The observation that edeine, a drug that prevents 60S binding to the 48S complex, induces SGs (31) also supports this proposition. SGs may be a product of a translational “checkpoint” that exists to monitor the integrity of this process. Once formed, the translation machinery remains

dynamically associated with SGs until the checkpoint signal is removed, *i.e.* disappearance of stress.

In addition to proteins involved in protein translation and RNA metabolism, SGs have been shown to sequester proteins in various important cellular processes. For example, stressed cells quickly sequester TRAF2 into SGs through interaction with eIF4G, which perturbs the signaling pathway from tumor necrosis factor  $\alpha$  to NF- $\kappa$ B (7). The junctional plaque protein plakophilin 3 (PKP3), an architectural component of desmosomes, is associated with SGs under stress conditions (32). Different regions of the rat hippocampus have different recoverability of SGs during reperfusion, and this correlates with

inhibition of translation initiation (33). These reports suggest that SGs may play diverse and important roles in different physiological or environmental stresses. The ability of arsenite to inhibit protein translation and cause SG formation, which eventually leads to the induction of apoptosis, has been exploited for the treatment of acute promyelocytic leukemia for decades (34). The finding that B-PatA localized within SGs accentuates the utility of small molecule natural products as tools to study biological phenomena. Not only will PatA and its analogs be useful tools for the study of cellular stress, they may also prove useful clinically.

*Acknowledgments*—We thank Drs. Jon Lorsch, Paul Englund, Jerry Hart, Randy Reed, and Daniel Lane for generous provision of advice and access to special equipment. We thank Drs. Karen Browning, Jerry Pelletier, David Ron, and Jens Lykke-Andersen for plasmids and antibodies. We thank Dr. Jing Xu for assistance with preparation of the manuscript. We also thank an anonymous reviewer for making the “Experimental Procedures” section more complete by requesting the inclusion of catalog numbers of all antibodies used.

### REFERENCES

- Nover, L., Scharf, K. D., and Neumann, D. (1983) *Mol. Cell. Biol.* **3**, 1648–1655
- Anderson, P., and Kedersha, N. (2002) *Cell Stress Chaperones* **7**, 213–221
- Anderson, P., and Kedersha, N. (2002) *J. Cell Sci.* **115**, 3227–3234
- Anderson, P., and Kedersha, N. (2006) *J. Cell Biol.* **172**, 803–808
- Coller, J., and Parker, R. (2004) *Annu. Rev. Biochem.* **73**, 861–890
- Moeller, B. J., Cao, Y., Li, C. Y., and Dewhirst, M. W. (2004) *Cancer Cell* **5**, 429–441
- Kim, W. J., Back, S. H., Kim, V., Ryu, I., and Jang, S. K. (2005) *Mol. Cell. Biol.* **25**, 2450–2462
- Kedersha, N. L., Gupta, M., Li, W., Miller, I., and Anderson, P. (1999) *J. Cell Biol.* **147**, 1431–1442
- Merrick, W. C. (2004) *Gene* **332**, 1–11
- Gingras, A. C., Raught, B., and Sonenberg, N. (1999) *Annu. Rev. Biochem.* **68**, 913–963
- McEwen, E., Kedersha, N., Song, B., Scheuner, D., Gilks, N., Han, A., Chen, J. J., Anderson, P., and Kaufman, R. J. (2005) *J. Biol. Chem.* **280**, 16925–16933
- Kedersha, N., Chen, S., Gilks, N., Li, W., Miller, I. J., Stahl, J., and Anderson, P. (2002) *Mol. Biol. Cell* **13**, 195–210
- McInerney, G. M., Kedersha, N. L., Kaufman, R. J., Anderson, P., and Liljestrom, P. (2005) *Mol. Biol. Cell* **16**, 3753–3763
- Kedersha, N., Cho, M. R., Li, W., Yacono, P. W., Chen, S., Gilks, N., Golan, D. E., and Anderson, P. (2000) *J. Cell Biol.* **151**, 1257–1268
- Gilks, N., Kedersha, N., Ayodele, M., Shen, L., Stoecklin, G., Dember, L. M., and Anderson, P. (2004) *Mol. Biol. Cell* **15**, 5383–5398
- Tourriere, H., Chebli, K., Zekri, L., Courselaud, B., Blanchard, J. M., Bertrand, E., and Tazi, J. (2003) *J. Cell Biol.* **160**, 823–831
- Bordeleau, M. E., Matthews, J., Wojnar, J. M., Lindqvist, L., Novac, O., Jankowsky, E., Sonenberg, N., Northcote, P., Teesdale-Spittle, P., and Pelletier, J. (2005) *Proc. Natl. Acad. Sci. U. S. A.* **102**, 10460–10465
- Low, W. K., Dang, Y., Schneider-Poetsch, T., Shi, Z., Choi, N. S., Merrick, W. C., Romo, D., and Liu, J. O. (2005) *Mol. Cell* **20**, 709–722
- Romo, D., Rzaia, R. M., Shea, H. A., Park, K., Langenhan, J. M., Sun, L., Akhizer, A., and Liu, J. O. (1998) *J. Am. Chem. Soc.* **120**, 12237–12254
- Mazan-Mamczarz, K., Lal, A., Martindale, J. L., Kawai, T., and Gorospe, M. (2006) *Mol. Cell Biol.* **26**, 2716–2727
- Fechir, M., Linker, K., Pautz, A., Hubrich, T., and Kleinert, H. (2005) *Cell Mol. Biol.* **51**, 299–305
- Scheuner, D., Song, B., McEwen, E., Liu, C., Laybutt, R., Gillespie, P., Saunders, T., Bonner-Weir, S., and Kaufman, R. J. (2001) *Mol. Cell* **7**, 1165–1176
- Kedersha, N., Stoecklin, G., Ayodele, M., Yacono, P., Lykke-Andersen, J., Fitzler, M. J., Scheuner, D., Kaufman, R. J., Golan, D. E., and Anderson, P. (2005) *J. Cell Biol.* **169**, 871–884
- Novac, O., Guenier, A. S., and Pelletier, J. (2004) *Nucleic Acids Res.* **32**, 902–915
- Anthony, D. D., and Merrick, W. C. (1992) *J. Biol. Chem.* **267**, 1554–1562
- Thompson, D. J. (1993) *Chem. Biol. Interact.* **88**, 89–114
- Bredfeldt, T. G., Kopplin, M. J., and Gandolfi, A. J. (2004) *Toxicol. Appl. Pharmacol.* **198**, 412–418
- Bode, A. M., and Dong, Z. (2002) *Crit. Rev. Oncol. Hematol.* **42**, 5–24
- Cavigelli, M., Li, W. W., Lin, A., Su, B., Yoshioka, K., and Karin, M. (1996) *EMBO J.* **15**, 6269–6279
- Bernstam, L., and Nriagu, J. (2000) *J. Toxicol. Environ. Health B Crit. Rev.* **3**, 293–322
- Thomas, M. G., Martinez Tosar, L. J., Loschi, M., Pasquini, J. M., Correale, J., Kindler, S., and Boccaccio, G. L. (2005) *Mol. Biol. Cell* **16**, 405–420
- Hofmann, I., Casella, M., Schnolzer, M., Schlechter, T., Spring, H., and Franke, W. W. (2006) *Mol. Biol. Cell* **17**, 1388–1398
- Kayali, F., Montie, H. L., Rafols, J. A., and DeGracia, D. J. (2005) *Neuroscience* **134**, 1223–1245
- Shen, Z. X., Chen, G. Q., Ni, J. H., Li, X. S., Xiong, S. M., Qiu, Q. Y., Zhu, J., Tang, W., Sun, G. L., Yang, K. Q., Chen, Y., Zhou, L., Fang, Z. W., Wang, Y. T., Ma, J., Zhang, P., Zhang, T. D., Chen, S. J., Chen, Z., and Wang, Z. Y. (1997) *Blood* **89**, 3354–3360

---

**Mechanisms of Signal Transduction:  
Eukaryotic Initiation Factor 2 $\alpha$   
-independent Pathway of Stress Granule  
Induction by the Natural Product  
Pateamine A**

Yongjun Dang, Nancy Kedersha, Woon-Kai  
Low, Daniel Romo, Myriam Gorospe, Randal  
Kaufman, Paul Anderson and Jun O. Liu  
*J. Biol. Chem.* 2006, 281:32870-32878.

doi: 10.1074/jbc.M606149200 originally published online September 2, 2006

---

Access the most updated version of this article at doi: [10.1074/jbc.M606149200](https://doi.org/10.1074/jbc.M606149200)

Find articles, minireviews, Reflections and Classics on similar topics on the [JBC Affinity Sites](#).

Alerts:

- [When this article is cited](#)
- [When a correction for this article is posted](#)

[Click here](#) to choose from all of JBC's e-mail alerts

Supplemental material:

<http://www.jbc.org/content/suppl/2006/09/06/M606149200.DC1.html>

This article cites 34 references, 19 of which can be accessed free at  
<http://www.jbc.org/content/281/43/32870.full.html#ref-list-1>